

A total of 44 genesets were significant. (orange/blue dot)

\* Threshold for significance:  $|\triangle \text{ GSVA score}| > 0.3$  & P-value  $< 0.05$

**(B)**

| Class                             | Gene set name                                       | High risk<br>(avg GSVA<br>score) | Non-high risk<br>(avg GSVA<br>score) | diff.score | T-stat. | P-value | FDR   |
|-----------------------------------|---|----------------------------------|--------------------------------------|------------|---------|---------|-------|
| Activated<br>In high risk group   | CROONQUIST_STROMAL_STIMULATION_DN                   | 0.278                            | -0.130                               | 0.408      | 4.604   | 0.000   | 0.112 |
|                                   | INAMURA_LUNG_CANCER_SCC_SUBTYPES_UP                 | 0.175                            | -0.147                               | 0.322      | 4.346   | 0.000   | 0.147 |
|                                   | chr9p   | 0.263                            | -0.118                               | 0.381      | 3.866   | 0.000   | 0.271 |
|                                   | BALLIF_DEVELOPMENTAL_DISABILITY_P16_P12_DELETION    | 0.214                            | -0.111                               | 0.325      | 3.814   | 0.001   | 0.292 |
|                                   | GO_POLY_A_MRNA_EXPORT_FROM_NUCLEUS                  | 0.132                            | -0.170                               | 0.301      | 3.321   | 0.003   | 0.452 |
|                                   | INAMURA_LUNG_CANCER_SCC_SUBTYPES_DN                 | 0.251                            | -0.139                               | 0.390      | 3.095   | 0.004   | 0.499 |
|                                   | chr19p  | 0.206                            | -0.158                               | 0.364      | 3.122   | 0.004   | 0.499 |
|                                   | BIOCARTA_TALL1_PATHWAY                              | 0.215                            | -0.094                               | 0.309      | 3.095   | 0.004   | 0.499 |
|                                   | BRUNEAU_SEPTATION_ATRIAL                            | 0.272                            | -0.119                               | 0.391      | 2.722   | 0.010   | 0.609 |
|                                   | GO_REGULATION_OF_MHC_CLASS_II BIOSYNTHETIC_PROCESS  | 0.220                            | -0.094                               | 0.314      | 2.759   | 0.011   | 0.627 |
|                                   | chr18p  | 0.297                            | -0.108                               | 0.405      | 2.682   | 0.011   | 0.635 |
|                                   | GO_MRNA_CLEAVAGE_AND_POLYADENYLATION_SPECIFICITY_FA | 0.111                            | -0.198                               | 0.308      | 2.595   | 0.016   | 0.690 |
|                                   | CTOR_COMPLEX  |                                  |                                      |            |         |         |       |
|                                   | LI_WILMS_TUMOR_ANAPLASTIC_DN                        | 0.251                            | -0.095                               | 0.346      | 2.471   | 0.020   | 0.703 |
|                                   | GO_REGULATION_OF_INTERFERON_GAMMA_SECRETION         | 0.239                            | -0.100                               | 0.340      | 2.382   | 0.026   | 0.734 |
|                                   | REACTOME_PROCESSING_OF_INTRONLESS_PRE_MRNAS         | 0.093                            | -0.211                               | 0.304      | 2.349   | 0.027   | 0.735 |
| Inactivated<br>In high risk group | RUNNE_GENDER_EFFECT_UP                              | 0.251                            | -0.112                               | 0.364      | 2.261   | 0.031   | 0.748 |
|                                   | FINETTI_BREAST_CANCER_KINOME_GREEN                  | 0.259                            | -0.081                               | 0.340      | 2.239   | 0.035   | 0.750 |
|                                   | MODULE_73   | 0.241                            | -0.083                               | 0.324      | 2.221   | 0.036   | 0.751 |
|                                   | BASSO_HAIRY_CELL_LEUKEMIA_DN                        | 0.188                            | -0.131                               | 0.319      | 2.150   | 0.040   | 0.760 |
|                                   | chryq11   | 0.231                            | -0.097                               | 0.328      | 2.090   | 0.044   | 0.763 |
|                                   | chr7p21   | -0.238                           | 0.090                                | -0.328     | -5.267  | 0.000   | 0.083 |
|                                   | chr17p12  | -0.222                           | 0.109                                | -0.331     | -4.941  | 0.000   | 0.083 |
|                                   | GO_G_PROTEIN_COUPLED_PHOTORECEPTOR_ACTIVITY         | -0.303                           | 0.201                                | -0.504     | -4.605  | 0.000   | 0.112 |
|                                   | HESSON_TUMOR_SUPPRESSOR_CLUSTER_3P21_3              | -0.340                           | 0.164                                | -0.504     | -4.708  | 0.000   | 0.112 |
|                                   | TESAR_ALK_TARGETS_EPISC_3D_UP                       | -0.249                           | 0.117                                | -0.366     | -4.322  | 0.000   | 0.161 |
|                                   | chr6q13   | -0.179                           | 0.150                                | -0.328     | -4.268  | 0.000   | 0.161 |
|                                   | chr11q25  | -0.286                           | 0.114                                | -0.400     | -4.311  | 0.000   | 0.161 |
|                                   | GO_GANGLIOSIDE_BIOSYNTHETIC_PROCESS                 | -0.174                           | 0.128                                | -0.302     | -4.083  | 0.000   | 0.288 |
|                                   | GO_KETONE_BODY_METABOLIC_PROCESS                    | -0.259                           | 0.122                                | -0.381     | -3.579  | 0.001   | 0.348 |
|                                   | REACTOME_OPSINS                                     | -0.278                           | 0.217                                | -0.495     | -3.383  | 0.002   | 0.406 |
|                                   | MIKHAYLOVA_OXIDATIVE_STRESS_RESPONSE_VIA_VHL_UP     | -0.218                           | 0.107                                | -0.325     | -3.228  | 0.002   | 0.453 |
|                                   | NIKOLSKY_BREAST_CANCER_17P11_AMPLICON               | -0.208                           | 0.142                                | -0.351     | -3.302  | 0.003   | 0.453 |
|                                   | GO_PREPULSE_INHIBITION                              | -0.154                           | 0.152                                | -0.305     | -3.300  | 0.003   | 0.467 |
|                                   | VANDESLUIS_NORMAL_EMBRYOS_UP                        | -0.264                           | 0.128                                | -0.391     | -3.193  | 0.003   | 0.467 |
|                                   | GO_INTRACILIARY_TRANSPORT_PARTICLE_B                | -0.220                           | 0.107                                | -0.327     | -3.154  | 0.004   | 0.499 |
|                                   | SCHAEFFER_PROSTATE_DEVELOPMENT_AND_CANCER_BOX5_DN   | -0.191                           | 0.131                                | -0.323     | -3.004  | 0.005   | 0.534 |
|                                   | chr6q26   | -0.189                           | 0.179                                | -0.368     | -2.984  | 0.006   | 0.534 |
|                                   | REACTOME_MITOCHONDRIAL_FATTY_ACID_BETA_OXIDATION    | -0.232                           | 0.136                                | -0.368     | -2.777  | 0.010   | 0.601 |
|                                   | CASTELLANO_HRAS_TARGETS_UP                          | -0.238                           | 0.085                                | -0.322     | -2.663  | 0.011   | 0.634 |
|                                   | GO_MEMBRANE_ASSEMBLY                                | -0.155                           | 0.155                                | -0.311     | -2.716  | 0.012   | 0.640 |
|                                   | MODULE_101  | -0.223                           | 0.102                                | -0.325     | -2.629  | 0.013   | 0.656 |
|                                   | GO_CELLULAR_RESPONSE_TO_NITROGEN_LEVELS             | -0.111                           | 0.209                                | -0.320     | -2.466  | 0.020   | 0.702 |
|                                   | CLIMENT_BREAST_CANCER_COPY_NUMBER_DN                | -0.156                           | 0.179                                | -0.335     | -2.473  | 0.021   | 0.714 |
|                                   | CHEN_HOXA5_TARGETS_6HR_DN                           | -0.245                           | 0.066                                | -0.311     | -2.155  | 0.040   | 0.757 |

**Figure S5.** (A) Volcano plot representing the result of GSVA. Orange and blue dots indicate significantly activated and inactivated gene-sets, respectively, in high risk group. (B) Among 17,810 gene sets from MsigDB, a total of 44 gene sets showed significant association with the risk group. The significance was determined by two-group T-test (P-value  $< 0.05$ ) and difference of average GSVA score between risk-groups  $> 0.3$ .

(C)

| Class                    | Gene set name   | High risk<br>(avg. GSVA<br>score) | Non-high risk<br>(avg. GSVA<br>score) | diff.score | T-stat. | P-value |
|--------------------------|---|-----------------------------------|---------------------------------------|------------|---------|---------|
| Activated in high risk   | GO_POLY_A_MRNA_EXPORT_FROM_NUCLEUS                              | 0.132                             | -0.170                                | 0.301      | 3.321   | 0.003   |
|                          | REACTOME_PROCESSING_OF_INTRONLESS_PRE_MRNAs                     | 0.093                             | -0.211                                | 0.304      | 2.349   | 0.027   |
|                          | GO_MRNA_CLEAVAGE_AND_POLYADENYLATION_SPECIFICITY_FACTOR_COMPLEX | 0.111                             | -0.198                                | 0.308      | 2.595   | 0.016   |
|                          | BIOCARTA_TALL1_PATHWAY  | 0.215                             | -0.094                                | 0.309      | 3.095   | 0.004   |
|                          | GO_REGULATION_OF_MHC_CLASS_II BIOSYNTHETIC_PROCESS              | 0.220                             | -0.094                                | 0.314      | 2.759   | 0.011   |
|                          | GO_REGULATION_OF_INTERFERON_GAMMA_SECRETION                     | 0.239                             | -0.100                                | 0.340      | 2.382   | 0.026   |
| Inactivated in high risk | GO_G_PROTEIN_COUPLED_PHOTORECEPTOR_ACTIVITY                     | -0.303                            | 0.201                                 | -0.504     | -4.605  | 0.000   |
|                          | REACTOME_OPSINS   | -0.278                            | 0.217                                 | -0.495     | -3.383  | 0.002   |
|                          | GO_KETONE_BODY_METABOLIC_PROCESS                                | -0.259                            | 0.122                                 | -0.381     | -3.579  | 0.001   |
|                          | REACTOME_MITOCHONDRIAL_FATTY_ACID_BETA_OXIDATION                | -0.232                            | 0.136                                 | -0.368     | -2.777  | 0.010   |
|                          | GO_INTRACILIARY_TRANSPORT_PARTICLE_B                            | -0.220                            | 0.107                                 | -0.327     | -3.154  | 0.004   |
|                          | GO_CELLULAR_RESPONSE_TO_NITROGEN_LEVELS                         | -0.111                            | 0.209                                 | -0.320     | -2.466  | 0.020   |
|                          | GO_MEMBRANE_ASSEMBLY  | -0.155                            | 0.155                                 | -0.311     | -2.716  | 0.012   |
|                          | GO_PREPULSE_INHIBITION  | -0.154                            | 0.152                                 | -0.305     | -3.300  | 0.003   |
|                          | GO_GANGLIOSIDE BIOSYNTHETIC_PROCESS                             | -0.174                            | 0.128                                 | -0.302     | -4.083  | 0.000   |

(D)

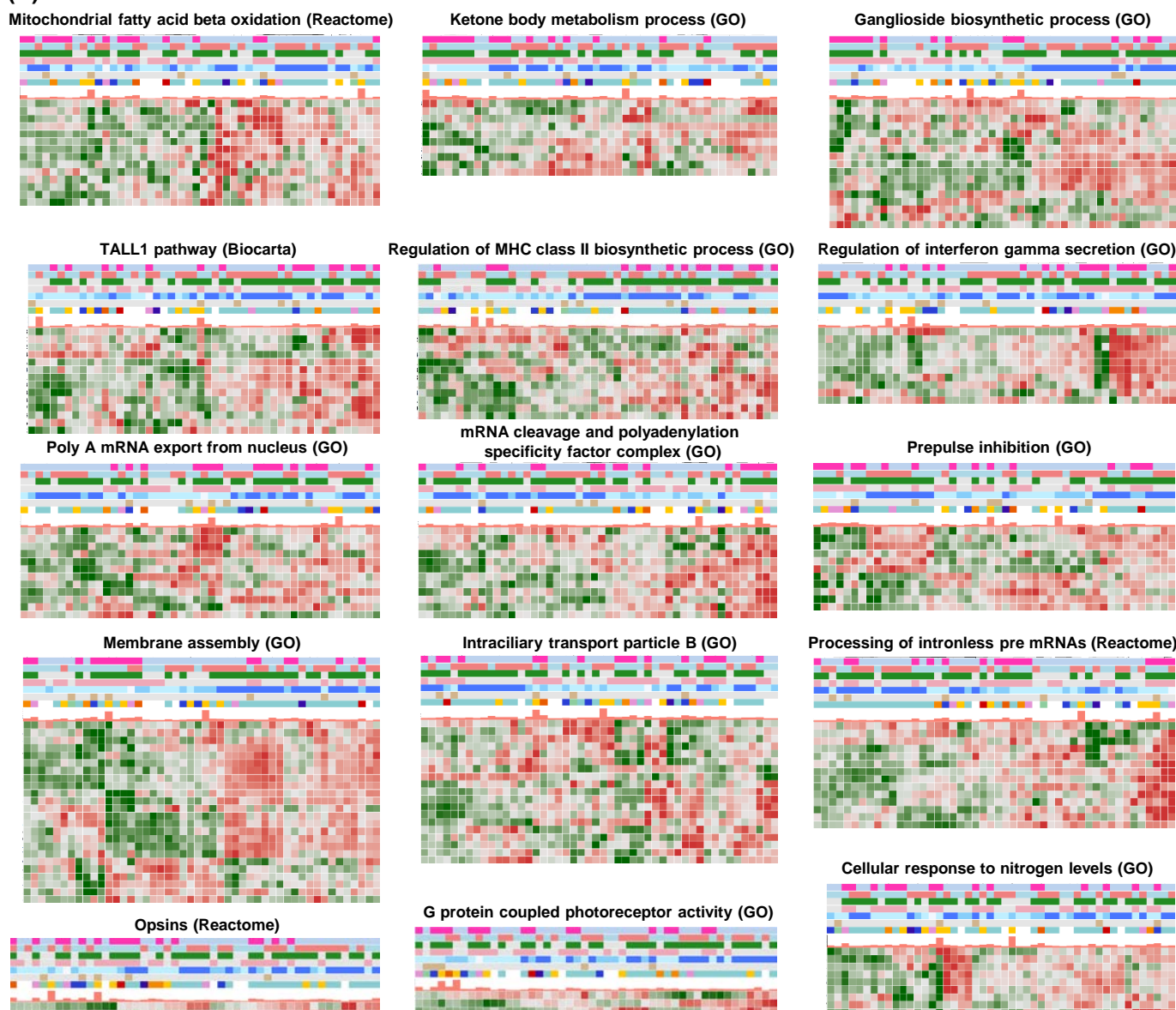


**Figure S5.** (C) The canonical pathways ( $n = 15$ ) that were significantly associated with risk groups were obtained from REACTOME, BIOCARTA, KEGG and GO databases. None of pathways were significant after adjusting  $P$ -values with FDR. (D) Gene expression profiles of the pathways showing significant association to risk groups.

(E)

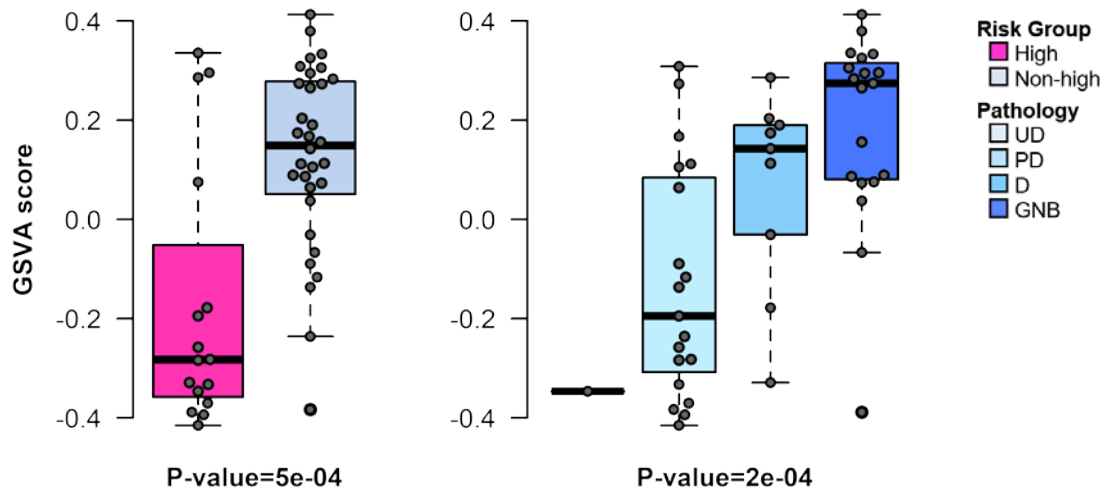


**Figure S5.** (E) The association of GSVA score of ganglioside biosynthesis pathway with risk-group (left) and pathology (right).